

Effect of hard processes on momentum correlations in pp and $p\bar{p}$ collisions

Guy Paic

Instituto de Ciencias Nucleares, UNAM, Mexico City, Mexico

Piotr Krzysztof Skowroński

*CERN, CH-1211 Geneva 23, Switzerland and
Warsaw University of Technology, Faculty of Physics,
ul. Koszykowa 75, 00-662 Warsaw, Poland*

2 April 2005

Abstract

The HBT radii extracted in $p\bar{p}$ and pp collisions at SPS and Tevatron show a clear correlation with the charged particle rapidity density. We propose to explain the correlation using a simple model where the distance from the initial hard parton-parton scattering to the hadronization point depends on the energy of the partons emitted. Since the particle multiplicity is correlated with the mean energy of the partons produced we can explain the experimental observations without invoking scenarios that assume a thermal fireball. The model has been applied with success to the existing experimental data both in the magnitude and the intensity of the correlation. As well, the model has been extended to pp collisions at the LHC energy of 14 TeV. The possibilities of a better insight into the string spatial development using 3D HBT analysis is discussed.

1 Introduction

The size of the source created in pp and $p\bar{p}$ collisions, as measured with momentum correlations, increases with the particle multiplicity ([1],[2]). The correlation of the extracted size with the rapidity density of the collisions, from the HBT analysis, was sometimes described as evidence for the existence of a "source" with a given size. Some alternative explanations have been given invoking long lived resonances and multiple parton interactions [3].

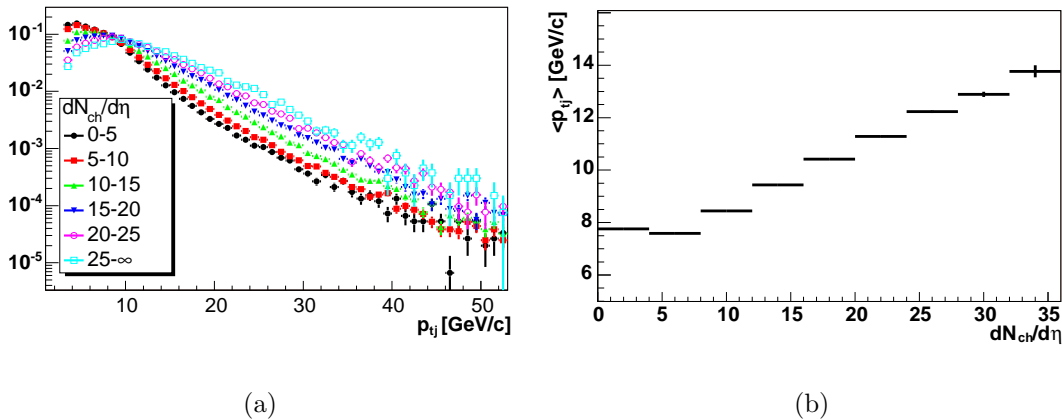


Figure 1: a) Distribution of the transverse jet momentum, for different $dN_{ch}/d\eta$ ranges. The cut at 3 GeV/c applied in the calculations is visible in the figure. b) Distribution of the mean transverse jet momentum (p_{tj}) versus $dN_{ch}/d\eta$. The results were obtained with Pythia at $\sqrt{s} = 1.8$ TeV.

In the present work we are investigating whether the observed behavior may be understood in terms of more trivial explanations related to the details of the hadronization of the partons leading to jets. We know namely, that the point of hadronization of a jet and the point of the initial parton-parton hard scattering do not coincide. The distance between them is the so called hadronization length (L_{hadr}).

Numerical estimates for the time scale of hadronization vary significantly [4],[5],[6], but owing to the Lorentz boost to the laboratory frame, they are proportional to the energy, $L_{hadr} \sim O(1)E_t$ ([7]). Hence, there is a dependence of L_{hadr} on the energy due to the Lorentz boost. On the other hand the energy spectrum of the emitted jets depends on the charged particle multiplicity of the events as shown in Fig.1. Hence if we assume that the hadronization occurs at different distances from the initial hard scatterings, depending on the energy of the jet, we can expect that this effect may simulate an extended hadronic source without invoking the presence of a thermalized source of hadrons. We have followed this line of thought in the present work.

2 Simulation

The simulation comprises three steps:

1. The simulation of the particle momenta using a standard Pythia event generator. Identification of jets and "underlying event".

2. Creation of a spatial distribution of particle origins according to our perception of the hadronization process.
3. Implementation of the Bose-Einstein effect and creation of the correlation functions.

2.1 Event generation and jets identification

With Pythia 6.24 [8] we simulate pp collisions with $\sqrt{s} = 1.8$ TeV. The PYCELL subroutine, that is part of the generator, is used to identify jets. We applied the following parameters:

- pseudo-rapidity range (η): from -2 to 2
- number of pseudo-rapidity bins: 1200
- number of bins in azimuthal angle: 1200
- threshold transverse energy of particles considered: 0
- minimum transverse energy of particles that are used as jet seeds: 0.7 GeV
- minimum jet transverse energy: 3 GeV
- maximum jet radius $R = \sqrt{\Delta\phi^2 + \Delta\eta^2}$: 1

All particles that do not belong to any jet are treated as an "underlying event". Jet axis \vec{p}_j - the direction along which the jet develops - is defined as

$$p_{tj} = \sum_i p_{ti} \quad (1)$$

$$\phi_j = \frac{\sum_i \phi_i p_{ti}}{p_{tj}} \quad (2)$$

$$\eta_j = \frac{\sum_i \eta_i p_{ti}}{p_{tj}} \quad (3)$$

$$\vec{p}_j = (p_{xj}, p_{yj}, p_{zj}) = p_{tj}(\cos \phi_j, \sin \phi_j, \sinh \eta_j) \quad (4)$$

The sums run over all particles that make up a jet. p_{ti} , ϕ_i and η_i are transverse momentum, azimuthal angle and pseudorapidity of the i th particle, respectively.

2.2 The Source Models

The events simulated with Pythia are then treated according to our model. Namely, the particles identified above as "underlying events" are given a spatial origin centered around the initial hard scattering point, while particles within a jet are given spatial coordinates of origin according to one of the models described below.

Tube It is assumed that the hadronization length (l_j , the distance from the hard scattering) depends linearly on the initial parton energy that we approximate by p_{tj} (jet total transverse momentum). Thus, $l_j = f_l p_{tj}$, where f_l is a multiplicative factor that represents our lack of theoretical insight into the process of hadronization. For every parton the loci of hadronization along the jet axis (x_l) is randomized from Gaussian distributions with a mean equal to l_j and a $\sigma_l = l_j/3$, preventing negative values. In the transverse direction (with respect to the jet axis) the hadronization points are randomized so that the distance to the jet axis follows a Gaussian distribution with a variance equal to σ_t and mean value of zero.

Dynamic width The distribution along the jet axis is the same as above while the transverse width σ_t depends linearly on the jet transverse energy and moreover, it is a function of the position along the jet axis (see Fig.2) so the distribution of hadronization points is:

$$\sigma_t(x_l, p_{tj}) = \begin{cases} \sigma_t^{\max} \exp \frac{-(l_j - x_l)^2}{w} & \text{if } \sigma_t^{\max} > \sigma_t^{\min} \\ \sigma_t^{\min} & \text{if } \sigma_t^{\max} \leq \sigma_t^{\min} \end{cases}, \quad (5)$$

where $\sigma_t^{\max} = f_l p_{tj}$, $\sigma_t^{\min} = 0.5$ fm and $w = \frac{l_j^2}{\ln 2 \sigma_t^{\max}}$ (w is chosen so $\sigma_t(x_l = 0)$ and $\sigma_t(x_l = 2l_j)$ are equal to σ_t^{\min}).

For both kinds of geometries the hadronization time is equal to x_l .

The positions of the "underlying event" particles are randomized from a single Gaussian distribution with variance σ_b . Their emission time is always equal to 0.

2.3 Simulation of BE correlations

Since the generator does not provide for Bose-Einstein correlations they have to be introduced. In our simulation we introduce them using the weighting algorithm due to Lednický [9]. It is applied during the construction of the correlation functions. Each particle pair (i, j) is weighted with a probability ρ_{ij}

$$C(Q, K) = \frac{1}{N(Q, K)} \sum_{(i, j)} \rho_{ij}, \quad (6)$$

$$\rho_{ij} = 1 + \cos((\mathbf{p}_i - \mathbf{p}_j) \cdot (\mathbf{x}_i - \mathbf{x}_j)). \quad (7)$$

where $N(Q, K)$ is the number of pairs in a given bin, $Q = p_i - p_j$ and $K = (p_i + p_j)/2$, \mathbf{x}_i and \mathbf{p}_i are the 4-vectors of the hadronization points and momentum in the pair rest frame, respectively. The probability ρ_{ij} coincides with the formal Born probability density $\Psi^* \Psi$ of the Bose-Einstein symmetrized 2-particle plane

wave.

$$\rho_{ij} = \Psi^*(\mathbf{x}_i, \mathbf{x}_j, \mathbf{p}_i, \mathbf{p}_j) \Psi(\mathbf{x}_i, \mathbf{x}_j, \mathbf{p}_i, \mathbf{p}_j), \quad (8)$$

$$\Psi(\mathbf{p}_i, \mathbf{p}_j, \mathbf{p}_i, \mathbf{p}_j) = \frac{1}{\sqrt{2}} \left(e^{i\mathbf{p}_i \mathbf{x}_i + i\mathbf{p}_j \mathbf{x}_j} + e^{i\mathbf{p}_j \mathbf{x}_i + i\mathbf{p}_i \mathbf{x}_j} \right). \quad (9)$$

2.4 Correlation Functions

The correlation functions are calculated for particles with $|\eta| < 1$ and $p_t > 0.1$ GeV, while no such a constraint is imposed in the jet finding procedure. We extract the correlation functions with two types of parameterizations.

- $C(Q_t, Q_0) = 1 + \lambda \exp\left(\frac{-1}{\hbar^2 c^2} (Q_t^2 R_t^2 + Q_0^2 \tau^2)\right)$
- $C(Q_{out}, Q_{side}, Q_{long}) = 1 + \lambda \exp\left(\frac{-1}{\hbar^2 c^2} (Q_{out}^2 R_{out}^2 + Q_{side}^2 R_{side}^2 + Q_{long}^2 R_{long}^2)\right)$

where:

- Q_t : is the component of the three-momentum difference perpendicular to the three-momentum sum
- Q_0 : is the difference of energies
- Q_{long} , Q_{out} and Q_{side} : are the components of 3-momentum difference vector in the Longitudinally Co-Moving System (LCMS). Q_{long} is parallel to beam, Q_{side} is perpendicular to beam and total pair momentum, and Q_{out} is perpendicular to Q_{long} and Q_{side} (Fig.2).
- R 's: corresponding radii
- τ : dispersion (radius) in the time domain

When speaking of the correlation function $C(Q_t)$ we mean the projection of $C(Q_t, Q_0)$ on the Q_t axis for $|Q_0| < 200$ MeV. By a double Gaussian fit we mean a 1D fit with the following form of a correlator

$$C(Q) = 1 + \lambda_1 e^{-\left(\frac{QR_1}{\hbar c}\right)^2} + \lambda_2 e^{-\left(\frac{QR_2}{\hbar c}\right)^2} \quad (10)$$

3 Results

The application of the model described above, in agreement with the intuition, shows that the correlation function indeed changes its shape with increasing multiplicity. Using the experimental data we have attempted to adjust the parameters of the model. We have fixed $\sigma_t = 0.5$ fm what corresponds to the typical hadronic size. We found that $\sigma_b = 0.4$ fm reproduces the experimental results at the lowest multiplicities (E735 has measured $R_t = 0.62$ fm at

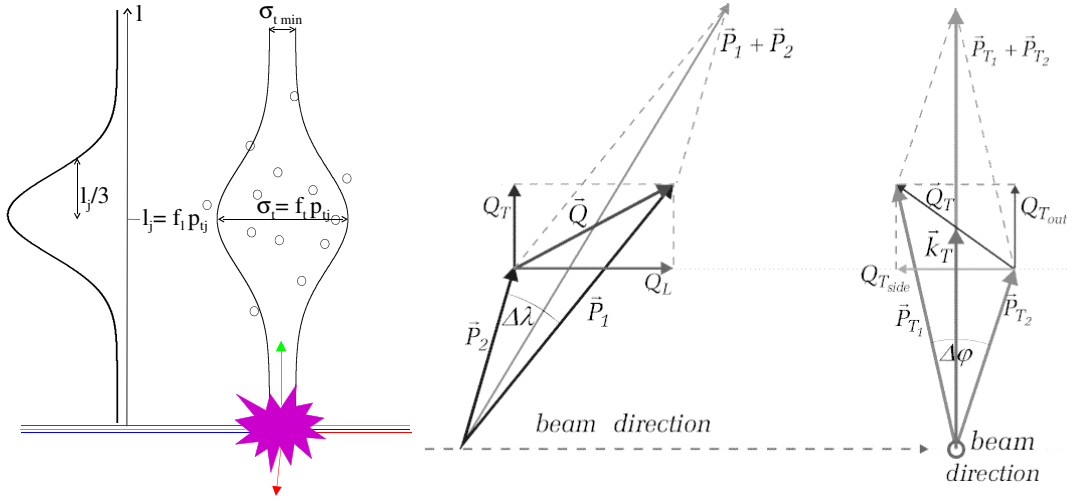


Figure 2: a) Schema of the the "dynamic width" jet geometry model. The spread in transverse direction with respect to the jet axis depends on the position along jet and its magnitude depends on the jet energy. b) Definition of Q_{out} , Q_{side} and Q_{long} .

$\langle dN_{ch}/d\eta \rangle = 6.75$). In the frame of our model it implies a non-negligible contribution of hard processes in total particle production even at low multiplicities. This observation is in an agreement with other observations at Tevatron [10].

However, we were not able to reach compatibility with the experimental values of R_t at high multiplicities. The increase of the f_l parameter causes a decrease of the intercept parameter, while the shape of the correlation function stays approximately unchanged. In fact, the width of the peak, thus R_t as given by a Gaussian fit even decreases with increasing f_l .

Using the *out-side-long* (OSL) parametrization we have observed that for this model R_{out} grows with f_l , while R_{side} stays approximately unchanged. This finding matches the intuitive representation. Therefore the applied geometry with a constant σ_t limits the growth of R_t . We deduce that R_{side} must also increase with the jet energy. This led us to the "dynamic width" jet geometry.

Using that model, we have found that we are able to reproduce the experimental results with $f_l = 1.0$ and $f_t = 0.6$, see Fig.6a and 4. This is not a unique pair of parameters that gives a good agreement with E735 result. Within some range we can decrease f_l and find such a value of f_t such that we still reproduce the experimental result (Fig.6b).

We believe that the precision on the determination of f values could be improved if results of a 3D HBT analysis were available. Namely, the dependence of R_{out} and R_{side} on event multiplicity is required. We have found that R_{side} increases together with f_t , and R_{out} together with f_l (see Table.1). It means

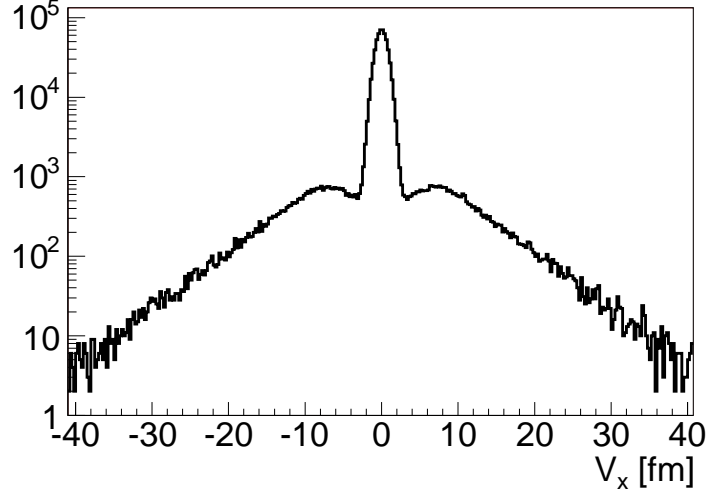


Figure 3: Cross-section through the 2D distribution of the hadronization points in the plane perpendicular to the beam. The difference in height between contributions from the "underlying event" (the peak for values around 0) and jets (shoulders) is a phase space effect. In fact, the majority of particles originate from jets. The dynamic width jet geometry with $f_l = 1.0$, $f_t = 0.6$ and $\langle dN_{ch}/d\eta \rangle = 12.4$.

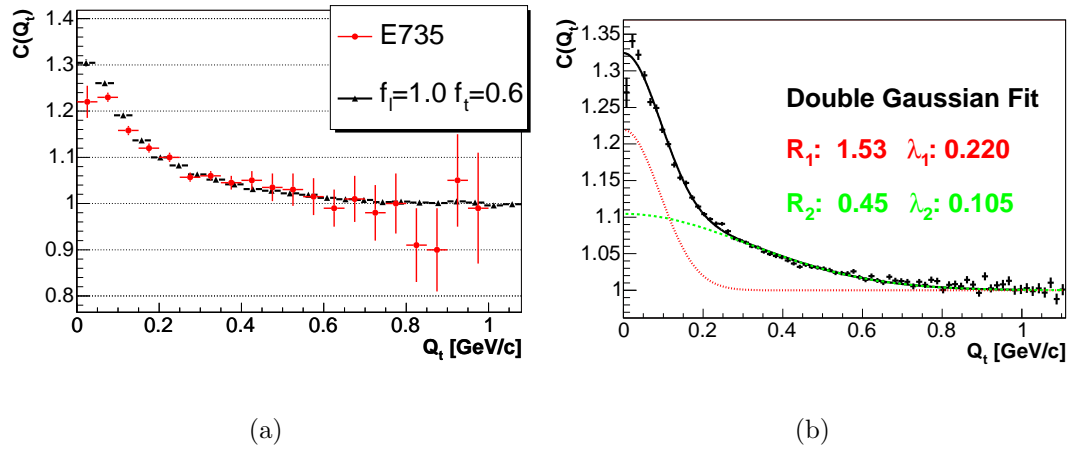
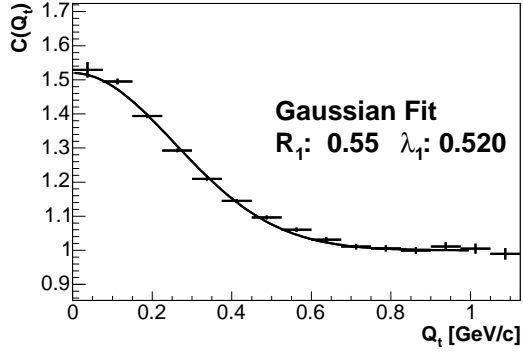
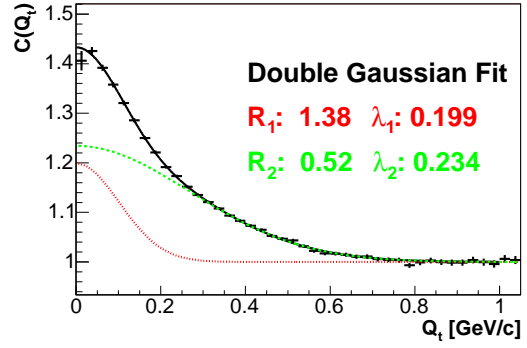


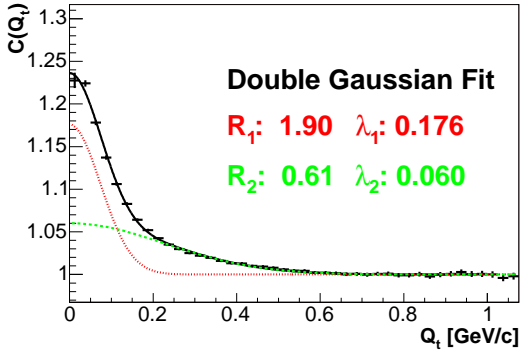
Figure 4: a) The Q_t correlation function from our model compared with the correlation function extracted from [2] ($\langle dN_{ch}/d\eta \rangle = 12.5$) and b) double Gaussian fit to it. The dynamic width jet geometry with $f_l = 1.0$, $f_t = 0.6$ and $\langle dN_{ch}/d\eta \rangle = 12.4$.



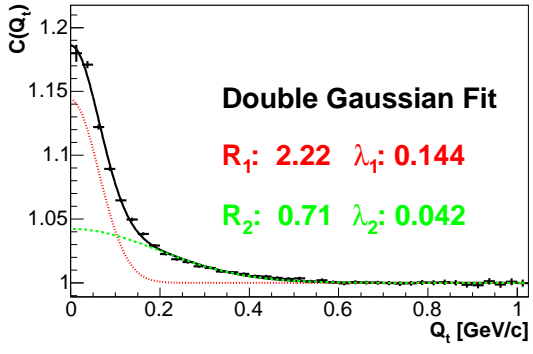
(a)



(b)



(c)



(d)

Figure 5: Q_t correlation functions for the case of the dynamic width geometry with $f_l = 1.0$ and $f_t = 0.6$ a) $dN_{ch}/d\eta = 3.2$, b) $dN_{ch}/d\eta = 7.3$, c) $dN_{ch}/d\eta = 17.2$, d) $dN_{ch}/d\eta = 23.0$

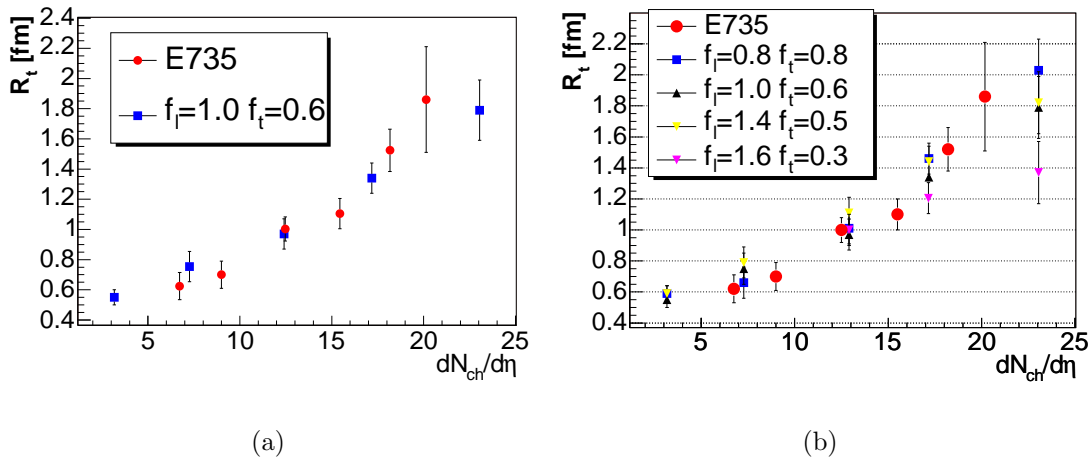


Figure 6: Results of our model compared to E735 result. The left hand plot shows the best fit to the data obtained with $f_l = 1$ and $f_t = 0.6$ while the right hand plot demonstrates the variation of the results with varying the f values.

that we can estimate the size of the jet fragmentation volume using the three dimensional correlation analysis.

In our model the "underlying event" (UE) is somewhat overestimated since we have imposed the cut on the jets of less than 3 GeV and this part has been added to the UE. We have examined how our results change if we reduce UE by removing randomly 50% of particles not assigned to jets. We have found that the obtained radii stay unchanged within 10%.

From Fig.7 we see that the correlation functions extend up to large Q 's (0.4 – 1.0 GeV), similarly to the ones obtained by E735. The slope of the "tail" depends on the multiplicity. The simulated correlation function cannot be well represented by a single Gaussian as expected from the distribution of particle hadronization points shown in Fig.3. As it can be seen e.g. in Fig.5c, a better fit of the correlation function is obtained using a double Gaussian, albeit it is not yet probably the exact form of a correlator for this kind of source. The two radii may be understood in term of the smaller one representing the correlations among the particles from the "underlying event" and the larger one representing the correlations of jet particles with the ones of the "underlying event", although the interplay of the different factors make such a representation only partially true.

It is important to mention that the extracted radii are much smaller than the extent of the source due to the fact that the particles from the "underlying event" are traveling while the jet did not yet hadronize! Similarly, particles hadronizing first within a jet also moves together with not yet hadronized partons. The same argumentation also explains the weak dependence of R_t on f_l in the "tube geometry".

f_l	f_t	R_{o1} [fm]	λ_1	R_{o2} [fm]	λ_2	R_{s1} [fm]	λ_1	R_{s2} [fm]	λ_2	R_{l1} [fm]	λ_1	R_{l2} [fm]	λ_2
0.2	0.2	0.82	0.55	-	-	1.33	0.61	-	-	1.28	0.58	-	-
0.25	0.25	0.92	0.50	-	-	1.51	0.55	-	-	1.44	0.53	-	-
0.3	0.3	1.02	0.47	-	-	1.65	0.52	-	-	1.56	0.50	-	-
0.4	0.4	2.12	0.23	0.84	0.23	2.02	0.44	0.51	0.03	2.42	0.40	0.75	0.09
0.5	0.5	2.30	0.24	0.79	0.19	2.22	0.42	0.40	0.03	2.47	0.37	0.61	0.08
0.6	0.6	2.70	0.19	0.87	0.17	2.77	0.31	1.01	0.08	3.11	0.28	1.04	0.12
0.8	0.8	2.88	0.21	0.67	0.11	2.84	0.28	0.69	0.05	3.41	0.25	0.84	0.09
1.0	0.6	3.03	0.25	0.66	0.11	2.75	0.28	0.67	0.06	3.00	0.27	0.78	0.09
1.4	0.5	3.52	0.25	0.64	0.09	2.55	0.26	0.75	0.06	2.89	0.23	0.86	0.09

Table 1: Dependence of OSL radii on f_l and f_t for the $\langle dN_{ch}/d\eta \rangle = 23.0$. The fits were made imposing a double Gaussian (Eq. 10) on 1D projections, taking two other components > 50 MeV. In the rows where R_2 is not specified fits did not converge and a single Gaussian is used instead.

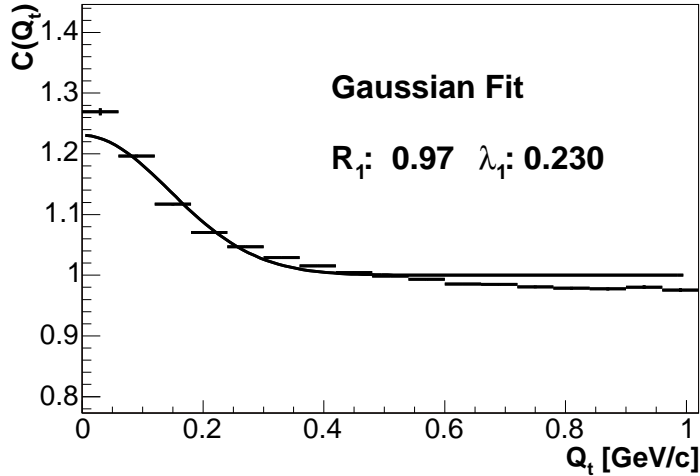


Figure 7: The same as in Fig.4, normalized at $Q_t \sim 500$ MeV and fitted with the single Gaussian form of the correlator.

$dN_{ch}/d\eta$	R_{t1} [fm]	λ_1	R_{t2} [fm]	λ_2
3.4	1.15	0.15	0.50	0.41
7.6	1.38	0.20	0.52	0.21
12.5	1.70	0.18	0.58	0.09
17.4	1.95	0.15	0.65	0.05
22.4	2.24	0.12	0.73	0.03
27.4	2.91	0.10	0.95	0.04
37.0	3.33	0.07	1.15	0.02

Table 2: R_t radii dependence on $dN_{ch}/d\eta$ at $\sqrt{s} = 14$ TeV, $f_l = 1.0$ and $f_t = 0.6$. The correlation functions were fitted with double Gaussian form of correlator (see Eq. 10).

Fitting such a correlation function with a single Gaussian - as was done in E735 - brings large uncertainties (Fig.7), because the obtained result is very sensitive to the normalization chosen (at which point correlation function crosses 1). To be able to compare with the experimental results [1][2] we have nevertheless used the single Gaussian fit. The results of the double Gaussian fits are shown in Fig. 4 and 5.

Finally we have calculated, using the parameters extracted for the Tevatron data, the expected correlation of radii with charged particle multiplicities for the maximum LHC energy of 14 TeV. In Table 2 we present results of our model obtained at LHC energies.

4 Conclusions

Using a simple approach which introduces a dependence of the distance of the mean hadronization points of a parton on its energy we have been able to reproduce very satisfactorily both the dependence of the radii, and the trend of the correlation strength lambda with the rapidity density in pp collisions. The present results indicate that there is a possibility of an alternative interpretation of the results to those presented in [2] and [12] where the obtained radii are interpreted as evidence for the observation of deconfined matter in pp collisions,

On the other hand the model a posteriori justifies the hadronization scenario envisaged because the free parameter f has been found close to unity for the range of multiplicities analyzed. We believe that the LHC with its wider range of multiplicities in pp collisions offers interesting possibilities to test our model. We have therefore presented here the expected variation of the radii in function of charged particle multiplicities at the LHC. Similarly, the effect of the parton hadronization should be taken into account in the analysis of HBT radii in heavy-

ion collisions [13].

5 Acknowledgments

We would like to acknowledge the very useful discussions with U. Wiedemann and J. Pluta.

References

- [1] UA1 Collaboration, *Phys. Lett. B* **226** (1989) 411
- [2] T. Alexopoulos *et al.*, *Phys. Rev. D* **48** (1993) 1931-1942
- [3] B. Buschbeck and H. C. Eggers, *Nucl. Phys. Proc. Suppl.* **92** (2001) 235
- [4] X. N. Wang, *Phys. Lett. B* 579 (2004) 299 [arXiv:nucl-th/0307036].
- [5] Y. L. Dokshitzer, V. A. Khoze, A. H. Mueller and S. T. Troyan, *Basics of Perturbative QCD*, Editions Frontières, France.
- [6] B. Z. Kopeliovich, *Phys. Lett. B* 243 (1990) 141.
- [7] U. A. Wiedemann, *J. Phys. G* **30** (2004) S649
- [8] T. Sjöstrand *et al.*, *Computer Phys. Commun.* **135** (2001) 238.
- [9] R. Lednický and V.L. Lyuboshitz, *Sov. J. Nucl. Phys.* **35**, 770 (1982); *Proc. CORINNE 90, Nantes, France, 1990* (ed. D. Ardouin, *World Scientific, 1990*) p. 42.
- [10] N. Moggi for the CDF Collaboration, FERMILAB-CONF-04-131-E *Presented at 12th International Workshop on Deep Inelastic Scattering (DIS 2004), Strbske Pleso, Slovakia, 14-18 Apr 2004*
- [11] P.K. Skowroński for ALICE Collaboration, [arXiv:physics/0306111].
- [12] L. Gutay [E-735 Collaboration], eConf **C030626** (2003) FRAP20 [arXiv:hep-ex/0309036]
- [13] G.Paić, P.K.Skowroński, B.Tomášik, *Nukleonika* **49** Suppl.2 (2004) 89 [arXiv:nucl-th/0403007]